Synthesis of Colloidal Silica Dumbbells

Patrick M. Johnson,*,†,‡ Carlos M. van Kats,† and Alfons van Blaaderen*,†

Soft Condensed Matter Group, Debye Institute, Utrecht University, Princetonplein 5, 3584 CC Utrecht, The Netherlands, and Physics Department, Simmons College, 300 The Fenway, Boston, Massachusetts 02446

Received July 11, 2005. In Final Form: September 13, 2005

We describe the synthesis and characterization of stable suspensions of monodisperse fluorescently labeled silica dumbbell particles. Pure dispersions of silica dumbbells with center-to-center lengths from 174 nm to 2.3 μm were produced with a variety of aspect ratios. Individual particles in concentrated dispersions of these particles could be imaged with confocal microscopy. These particles can be used as a colloidal model system for addressing fundamental questions about crystal and glass formation of low-aspect-ratio anisotropic particles. They also have potential in photonic applications and electro-optical devices.

I. Introduction

Recent fundamental studies have shown that a combination of index matching and fluorescent labeling makes it possible to quantitatively study the structure and dynamics of concentrated colloidal dispersions of spheres on a single-particle level with confocal microscopy.[1−5] The extensive knowledge that is available to modify the surface of silica and latex particles allows the tuning of interactions from long-range repulsive[6,7] to hard-sphere-like[1,2,8] to even dipolar.[9,10] Thus far, almost all such fundamental quantitative real-space studies have been carried out only using colloidal spheres. However, a number of theoretical and experimental results show the wide variety of novel structure and dynamics for monodisperse anisotropic systems.[11]

Experimental studies on anisotropic colloidal model systems have focused mainly on high-aspect-ratio particles. Examples of isotropic−nematic phase behavior have been observed with several different types of organic rods (FD-, TMV-virusses, Collagen, DNA,)[12−14] and inorganic materials (Vanadiumpentoxide (V_2O_5) β-ferric oxyhydroxide (β-FeOOH), boehmite (ALOOH)).[15−18] The first real-space observation of self-ordering behavior of liquid crystals from rodlike colloidal particles on a single-particle level has recently been reported by Maeda,[19] though the high refractive index of β-ferric oxyhydroxide will make it hard to extend these studies into three dimensions. We have recently shown that fluorescently labeled high-aspect-ratio silica rods, suitable for single-particle tracking via confocal microscopy and with a sufficiently high yield for phase behavior studies, can be synthesized.[20] Similarly, collective behavior and quantitative confocal imaging were reported by Solomon et al.[21] These authors made fluorescently labeled ellipsoidal PMMA particles with high aspect ratios by stretching colloidal particles in a polymer matrix above the glass temperature.[22]

Theories and simulations of low-aspect-ratio hard core particles have predicted new phases, including a plastic crystal phase,[23,24] and novel colloidal glass behavior.[25] These simulations also show that there is very little difference between the phase diagram of hard sphere dumbbells and that of hard spherocylinders of the same aspect ratio, suggesting that the exact shape may not be very important in this parameter region and that experimental results for low-aspect-ratio dumbbells may be representative for other particles such as spherocylinders.[24]" To experimentally test these theories, the synthesis of dispersions of anisotropic particles, properly labeled for confocal microscopy analysis, is essential. Such particles, with their optically anisotropic scattering properties and capacity to reorient in external fields, may also lead to new types of photonic materials.[26−28]

* To whom correspondence should be addressed. E-mail: patrick.johnson@simmons.edu (P.M.J.); A.vanBlaaderen@phys.uu.nl (A.v.B.).

† Utrecht University.

‡ Simmons College.

(1) van Blaaderen, A.; Wiltzius, P. *Science* **1995**, *270*, 1177.
(2) van Blaaderen, A.; Ruel, R.; Wiltzius, P. *Nature* **1997**, *385*, 321.
(3) Kegel, W. K.; van Blaaderen, A. *Science* **2000**, *287,* 290.
(4) Gasser, U.; Weeks, E. R.; Schofield, A.; Pusey, P. N.; Weitz, D. *Science* **2001**, *292*, 258.
(5) Yethiraj, A.; van Blaaderen, A. *Nature* **2003**, *421*, 513.
(6) van Blaaderen, A. *MRS Bull.* **1998**, *23*, 39.
(7) Hachisu, S.; Kobayashi, Y.; Kose, A. *J. Colloid Interface Sci.* **1973,** *42*, 342.
(8) Pusey, P. N.; Van Megen, W. *Nature* **1986**, *320*, 340.
(9) Dassanayake, U.; Fraden, S.; van Blaaderen, A. *J. Chem. Phys.* **2000**, *112*, 3851.
(10) Martin, J. E.; Odinek, J.; Halsey, T. C.; Kamien, R. *Phys. Rev. E* **1998**, *57*, 756.
(11) Lekkerkerker, H. N. W.; Vroege, G. J. Phase Transitions in Colloidal Dispersions. In *Fundamental Problems in Statistical Mechanics VIII*; van Beijeren, H., Ernst, M. H., Eds.; Elsevier Science: Amsterdam, 1994, p 207.
(12) Stroobants, A.; Lekkerkerker, H. N. W.; Odijk, T. *Macromolecules* **1986**, *19*, 2232.
(13) Fraden, S.; Maret, G.; Caspar, D. L. D.; Meyer, R. B. *Phys. Rev. Lett.* **1989**, *63,* 2068.
(14) Tracey, M. A.; Pecora, R. *Macromolecules* **1992**, *25*, 337.
(15) Pelletier, O.; Davidson, P.; Bourgeaux, C.; Livage, C. J. *Europhys. Lett.* **1999**, *48*, 53.
(16) Maeda, H.; Maeda, Y. *Langmuir* **1995**, *11*, 1446.
(17) Buining, P. A.; Philipse, A. P.; Lekkerkerker, H. N. W. *Langmuir* **1994**, *10*, 2106.
(18) van Bruggen, M. P. B.; Dhont, J. K. G.; Lekkerkerker, H. N. W. *Macromolecules* **1999**, *32*, 2256.
(19) Maeda, H.; Maeda, Y. *Phys. Rev. Lett.* **2003**, *90*, 18303.
(20) van Kats, C. M.; Johnson, P. M.; van den Meerakker, J. E. A. M.; van Blaaderen A. *Langmuir* **2004**, *20*, 11201.
(21) Mohraz, A.; Solomon, M. J. *Langmuir* **2005**, *21*, 5298.
(22) Ho, C. C.; Keller, A.; Odell, J. A.; Ottewill, R. H. *Colloid Polym. Sci.* **1993**, *271*, 47.
(23) Bolhuis, P.; Frenkel, D. *J. Chem. Phys.* **1997**, *106*, 666.
(24) Vega, C.; Monson, P. A. *J. Chem. Phys.* **1997**, *107*, 2696.
(25) Letz, M.; Schilling, R.; Latz, A. *Phys. Rev. E.* **2000**, *62*, 5173.
(26) Yin, Y.; Xia, Y. *Adv. Mater.* **2001**, *13*, 267.
(27) Velikov, K. P.; van Dillen, T.; Polman, A.; van Blaaderen, A. *Appl. Phys. Lett.* **2002**, *81*, 838.
(28) Birner, A.; Wehrspoon, R. B.; Goesele U. M.; Busch, K. *Adv. Mater.* **2001**, *13,* 377.

10.1021/la0518750 CCC: $30.25
Published on Web 10/20/2005

A few groups have reported methods to synthesize low-aspect-ratio anisotropic particles with relative standard deviations in size distributions below 20%. Recently, Manoharan et al. have synthesized and separated small quantities of identically arranged particles in conglomerates of up to 13 spheres by aggregating colloids attached to the interface of liquid droplets in an emulsion.[29] Yin et al. have been able to fuse spherical colloids on patterned substrates in small quantities.[30] Liddel et al. have synthesized high-refractive-index zinc sulfide dumbbell particles with the goal of creating new photonic crystal structures,[31] though such systems are less interesting as model systems since index matching is not feasible. Snoeks et al. have used ion beam irradiation to produce ellipsoidal colloids.[32]

In this article, we show how monodisperse anisotropic silica particles with aspect ratios below 2 and with fluorescently labeled cores can be synthesized. The particles are designed to allow real space analysis of anisotropic model systems and may also serve as components of novel materials based on colloidal crystals, such as photonic crystals.[33] The methods described in this paper are comparatively simple and can produce high yields of particles. Furthermore, the aspect ratio of these particles can be easily tuned.

Experimental Section

Anisotropic particles were formed by slightly destabilizing dispersions of spherical silica colloids to allow an initial stage of aggregation, i.e., dumbbell formation, to proceed. The process was terminated before significant amounts of aggregates composed of more particles had formed. The main method investigated in this article involved the use of shear-induced aggregation in ammonia/ethanol solutions (method 1) in which the silica particles were not completely stable. Following dumbbell formation, continuous growth of a silica layer in a seeded-growth step allowed the shape of the particle to be tuned, reducing the aspect ratio. We also present synthesis conditions and X-ray scattering results for pure dumbbell dispersions of much smaller particles synthesized from microemulsions for which the destabilizing mechanism is less well understood (method 2). For both methods, the dumbbells were separated from single spheres and larger aggregates via centrifugation techniques. The resulting dispersions contained pure dumbbells.

Chemicals. Ammonia (29.7% w/w of NH_3 in H_2O, Merck), fluoresceine isothiocyanate (FITC, Sigma), rhodamine B isothiocyanate (RITC, Aldrich), and 3-aminopropyltriethoxy silane (APS, Fluka) were used as received. Ethanol (absolute, technical grade, Lamers & Pleuger) and tetraethoxysilane (TEOS, Fluka) were freshly distilled before use. For the microemulsion synthesis, cyclohexane (p.a. Merck), Igepal CO-520 (np5, Aldrich) were used as received. Sucrose (Sigma), for density gradient centrifugation, and dimethyl sulfoxide (DMSO, Fluka), for index matching, were used as received. Molarities were calculated by assuming additivity of volumes of reagents/components.

Dumbbell Synthesis. The spherical fluorescent silica core−shell particles used as precursors for dumbbells made using method 1 were made following a two-step process as described by van Blaaderen et al.[34,35] The fluorescent core was synthesized by adding the reaction product of APS and FITC to a mixture of TEOS and ammonia in ethanol. APS (1.42 g, 6.41 mmol) was coupled to 244 mg of FITC (0.627 mmol) and stirred overnight in 10 mL of absolute ethanol. This mixture was added together with 70 mL of TEOS (0.31 mol) to a mixture of 175 mL of ammonia and 1750 mL of ethanol. The resulting cores radius was 200 nm with a polydispersity of 5%. These cores were grown further following a method described by Giesche.[36] Separate TEOS/ethanol and ammonia/water/ethanol feeds under nitrogen atmosphere were added dropwise to a 0.6 M silica suspension in ethanol containing 8.0 M water and 0.6 M NH_3 until the desired particle size was achieved. The TEOS/ethanol feed contained 2.0 M TEOS in ethanol. The ammonia/water/ethanol feed contained 1.2 M NH_3 and 16.0 M water in ethanol. This process resulted in spherical particles with FITC-labeled silica cores and unlabeled silica shells. The particles were transferred via repeated slow centrifugation (<120*g*) to 96% ethanol and could be stored indefinitely.

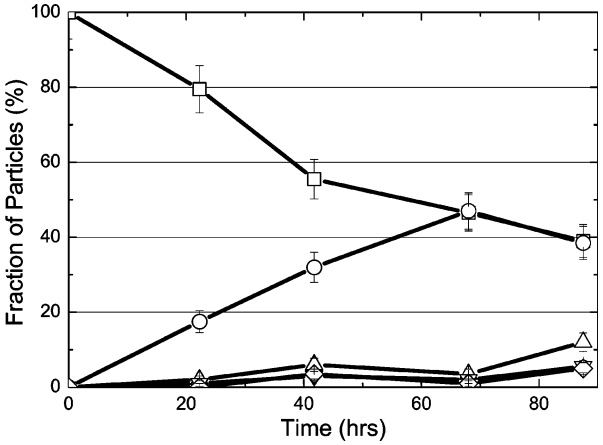

Figure 1. The fraction of aggregates of different sizes as a function of time in a dispersion of 1.4 μm colloids in 120 mL/L ammonia and ethanol under shear (orthokinetic aggregation). Particles composed of 1, 2, 3, 4, and 5 or more spheres have the symbols square, circle, triangle, inverted triangle, and diamond, respectively. The number of dumbbells peaks at an anomalously high 45% after 70 h, with few larger aggregates yet formed.

Method 1 involved destabilizing the particles through the addition of ammonia and then inducing aggregation through the application of shear (i.e., orthokinetic aggregation). Addition of ammonia increases both the surface charge of the colloids (at low ammonia concentrations), as well as the ion concentration. At high ammonia concentrations, the surface charge is no longer affected by the addition of ammonia, thus the increase of ionic strength is the main effect which destabilizes the silica spheres.

A high yield of dumbbells was obtained under the following synthesis conditions. Particles (1.4 μm diameter, 1.5% v/v) were dispersed in a mixture of 0.875 mL of ammonia and 6.12 mL of ethanol (ammonia 120 mL/L in ethanol). The dispersion was mixed in a cylindrical vial, 2 cm diameter, 5 cm length, which was rotated at 120 rpm horizontally on rollers with no stir bar (high but irreproducible dumbbell yields were also found using a stir bar rather than rollers.) Tests of lower ammonia concentrations (60 mL/L) using otherwise the same conditions produced lower dumbbell yields.

The number of dumbbells produced as a function of time was tracked by taking small samples from the metastable dispersion at various times during the synthesis, diluting these samples by a factor of 20 in ethanol to stabilize the particles, and analyzing the stabilized sample under a fluorescence microscope. By observing the particles in the bulk of the diluted sample (up to 100 μm from the wall) and randomly choosing particles visually, the fraction of singles, dumbbells, triplets, and larger clusters could be measured as a function of time (Figure 1). This process was also tested with an ammonia concentration of 60 mL/L; however, the resulting dumbbell formation rate was much slower and thus less ideal.

Much smaller silica dumbbells were also synthesized using a different method (method 2). First, small monodisperse spherical

(29) Manoharan V. N.; Elsesser M. T.; Pine D. J. *Science* **2003**, *301*, 483. Yi, G. R.; Manoharan, V. N.; Michel, E.; Elsesser, M. T.; Yang, S. M.; Pine, D. J. *Adv. Mater.* **2004**, *16*, 1204.

(30) Yin, Y.; Lu, Y.; Gates, B.; Xia, Y. *J. Am. Chem. Soc.* **2001**, *123*, 8718.

(31) Liddell C. M.; Summers, C. J. *Adv Mater* **2003**, *15*, 1715.

(32) Snoeks, E.; van Blaaderen A.; Van Dillen, T.; van Kats, C. M.; Brongersma, M. L.; Polman, A. *Adv. Mater.* **2000**, *12*, 1511.

(33) Vlasov, Y. A.; Xiang-Zheng, B.; Sturm, J. C.; Norris, D. J. *Nature* **2001**, *414*, 289.

(34) Verhaegh, N. A. M.; van Blaaderen, A. *Langmuir* **1994**, *10*, 1427.

(35) van Blaaderen, A.; van Geest, J.; Vrij, A. *J. Colloid Interface Sci.* **1992**, *154*, 481.

(36) Giesche, H. *J. Eur. Ceram. Soc.* **1994**, *94*, 189.

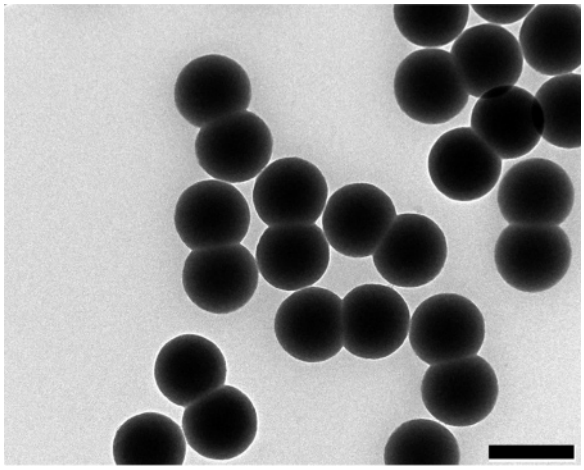

Figure 2. TEM image of the silica dumbbells formed from seed particles grown in a microemulsion and aggregated by depletion effects (method 2). The polydispersities in diameter and length are both extremely low (~1.5%), suggesting that this is an excellent method for producing monodisperse nanoscale dumbbells. The scale bar is 200 nm. Notice that overlapping particles (upper right) can be distinguished from dumbbell connections for particles of this size.

seed particles were synthesized in a water-in-oil microemulsion following the method of Osseo-Asare.[37] Forty one milliliters of Igepal CO520, a nonionic surfactant, was mixed with 800 mL cyclohexane. Ammonia (4.85 mL) was added, and the mixture stirred for 30 min to form a microemulsion. Then, 5.0 mL of TEOS (22 mmol) was added under slow stirring and temperature control (20 °C) to form monodisperse silica particles (radius ≈ 25 nm, polydispersity ≈ 3%). The reaction was completed after a week at constant (20 °C) temperature. One-third of these particles were grown to larger particles by first transferring the seed particles to a mixture of ethanol and ammonia. To this end, the cyclohexane was first removed by rotary evaporation and replaced with an equal amount of an ammonia in ethanol (100 mL/L) mixture. Then, TEOS was added in batches to grow the particles to a radius of 86 nm. The added TEOS did not exceed 40 mL/L per batchwise addition to avoid second nucleation. During this particle growth, dumbbells formed (Figure 2). The destabilizing mechanism may be a depletion-induced attraction driven by micelles formed by the surfactant molecules. However, further study is necessary to confirm this hypothesis.

Lowering the Size Ratio. Once the dumbbells were formed, additional layers of SiO_2 were added to tune the dumbbell aspect ratio. To this end, a seeded growth method similar to that of Giesche[36] was again used in order to avoid secondary nucleation of spheres and new dumbbell formation. In some of the samples, the large dumbbell seeds were mixed with small (300 nm diameter) silica spheres to prevent second nucleation (samples 1A_1 and 1B). In samples with higher concentrations of dumbbell seeds (samples 1C_1 and 1C_2), no additional small spheres were added. All of the seed solutions contained initial concentrations of 30 mL/L ammonia. A feed of diluted TEOS in ethanol was added dropwise to the dispersions over different periods of time to create different aspect ratios. For samples 1C_1 and 1C_2, a second ammonia/water/ethanol feed was added dropwise through separate tubes to maintain a constant molar concentration of NH_3 and water during the synthesis.[36] A complete list of synthesis conditions tested is given in Table 1.

One batch of dumbbells (sample 1B_3) was coated with an extra fluorescent layer to facilitate the tracking of particles with confocal microscopy. RITC (2.6 mg, 4.9 μmol) was mixed with 2.15 μL of APS (9.2 μmol) in 0.5 mL of 100% ethanol and stirred overnight to couple the RITC and APS. Nineteen microliters of this mixture was added simultaneously with 125 μL of TEOS batchwise to the dispersion. The same ammonia concentration (30 mL/L) was used. This was repeated two times to create a 20 nm layer of rhodamine-dyed silica.

The polydispersity for different synthesis conditions was measured using scanning electron microscopy (SEM) for the larger particles and transmission electron microscopy (TEM) for the smallest particles.

Purification of Dumbbells. Synthesis conditions were chosen such that the dispersions produced after aggregation and seeded growth were a mixture of single spheres, dumbbells, and relatively small amounts of clusters of three or more particles. To separate small amounts of dumbbells from the dispersion, two centrifugation techniques were used. Density gradient centrifugation[29,38] was used to create small yields of particles in one step. The gradient was created with a two-cylinder gradient-forming device (550 mL, Sigma-Aldrich). A Hettich Rotina 46S centrifuge with swing-out buckets was used at typical accelerations of 40−160g. Both sucrose−water and glycerol−water gradient mixtures were tested. The largest gradients used were 0.037 (g/mL)/cm. A wide centrifuge tube, with an inner diameter of 5.8 cm was used to maximize the yield. A thick (1/2 cm) band of colloids was loaded as an inverse gradient using the gradient-forming device. The maximum inverse gradient loaded was $|\partial f/\partial z|_{max} = 0.009\ cm^{-1}$, where f is the volume fraction of the colloids.

To achieve larger yields than with the density gradient method, repeated centrifugation in uniform solvents was also tested. Particles were centrifuged until dumbbells and larger aggregates had completely sedimented but a fraction of the spherical particles had not. The speed of dumbbell sedimentation was found to be

Table 1. Conditions for Seeded Growth[a]

	initial particle concn (v/v%)		TEOS/EtOH feed			
name (diameter (nm) of seeds)	dumbbell seeds	additional (d = 300 nm)	TEOS concn (v/v in EtOH)	rate (mL/h)/ (duration)	remark	new L, D
1A_1 (1400)	0.1	0.1	.05	1.7/(42 h)	small particles grown onto 10% of dumbbells	$D = 1770 \pm 2\%$ $L = 1400 \pm 6\%$
1A_2 (1770)	0.1	none	.05	1.7/(44 h)	2nd nucleation	$D = 2300 \pm 2\%$ $L = 1400 \pm 6\%$
1B_1 (1400)	0.1	0.1	.01	1.7/(35 h)		$D = 1500 \pm 2\%$ $L = 1400 \pm 2\%$
1B_2 (1500)	0.1	0.1	.01	1.7/(24 h)		$D = 1610 \pm 2\%$ $L = 1380 \pm 2\%$
1B_3 (1610)	.075 (60 mL)	none	TEOS and RITC added batchwise (see text)			$D = 1630 \pm 2\%$ $L = 1370 \pm 3\%$
1C_1 (1400)	0.88 (20 mL)	none	.05	1.17/(16 h)	2nd nucleation	$D = 1690 \pm 2\%$ $L = 1430 \pm 3\%$
1C_2 (1690)	0.75 (20 mL)	none	.025	1.15/(19.5 h)		$D = 1810 \pm 2\%$ $L = 1440 \pm 3\%$

[a] The starting dispersions consist of particles created via destabilization under shear flow (method 1), referred to as "dumbbell seeds", mixed in some cases with additional 300 nm diameter spheres. Successive samples with the same letter (for example 1B_1, 1B_2, and 1B_3) use the previous sample as a seed dispersion. The starting ammonia concentration for each sample was 30 mL/L. This concentration was held fixed for samples 1C_1 and 1C_2 by adding an additional ammonia/water/ethanol feed. The dumbbell particle dimensions given in the last column include an uncertainty that contains both the measurement uncertainty and the polydispersity. The measurement uncertainty of L was ~2%.

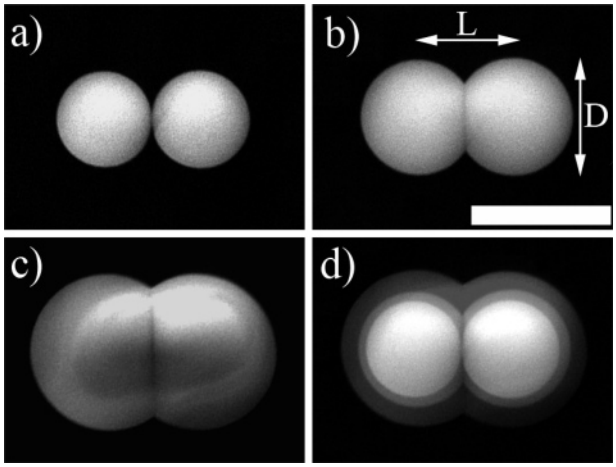

Figure 3. SEM image of dumbbell growth by TEOS addition. (a) $D = 1.40\ \mu$m, $L = 1.40\ \mu$m, (b) $D = 1.74\ \mu$m, $L = 1.40\ \mu$m (sample 1A_1), and (c) $D = 2.30\ \mu$m, $L = 1.40\ \mu$m (sample 1A_2). The initial dumbbell shown in (a) was formed by destabilizing the dispersion in ammonia under application of shear (method 1). Subsequent stages in the growth of the same dispersion are shown in (b) and (c). The images (a−c) are superimposed in image (d) to illustrate the uniformity of the layers grown. Image (b) includes arrows that give the definition of L and D used in this paper. The scale bar in the lower right of image (b) is 2 μm, which may be applied to all four images.

up to 1.35 that of the spherical particles depending on the aspect ratio. The timing of the centrifugation was chosen such that roughly 15% of the single spheres could be removed with each step. This method requires more than 20 repeated separations to purify the dumbbells but has the potential to produce higher yields than density gradient centrifugation.

Small-Angle X-Ray Scattering. Low concentrations of the 174 nm diameter dumbbells created with method 1 were analyzed using small-angle X-ray scattering (SAXS) at the European Synchrotron Radiation Facility (ESRF) in Grenoble, France (ESRF, BM26 DUBBLE-beamline). X-rays of wavelength 1.24 Å were recorded at an 8 m distance from the sample.

Confocal Microscopy. Dense sediments of pure dumbbell samples were analyzed on a single-particle level using confocal microscopy (Leica TCS SP2, 63×/N.A. 1.4 lens, 488 nm Ar/Kr excitation wavelength). Dispersions were prepared in an index of refraction matching solvent mixture (88% w/w DMSO/water) at 0.25% v/v colloid concentration. To use the minimum amount of sample, narrow sedimentation vials were built by affixing a 3 cm length, 1 mm diameter hollow glass cylinder (the top of a Pasteur pipet) to a glass cover slip such that the cylinder stood vertically when the cover slip was horizontal. Silicone rubber (GE) was used to glue the cylinder to the cover slip. These sample holders were filled with the index-matched dumbbell dispersion and mounted on an inverted scanning confocal microscope so that the colloids sedimented slowly onto the cover slip. In this way, sediments of 100−200 μm thick were slowly formed and were analyzed. Particle tracking was achieved using IDL (RSI) and methods similar to those described by van Blaaderen et al.[1,2] and Crocker and Grier.[39]

II. Results and Discussion

Figure 3 shows SEM images of dumbbells in various stages of growth with aspect ratios of 1.0 (Figure 3a), 0.80 (Figure 3b), and 0.61 (Figure 3c). Figure 3d shows a superposition of the dumbbells (sample 1A) in the three stages of growth. As this image shows, a uniform layer of silica was grown with each step. The dumbbell size and aspect ratio are defined by the diameter of the component spheres, D, and the center-to-center distance between the spheres, L (Figure 2b). The polydispersity of dumbbells is characterized by the standard deviations from the mean for D and L, i.e., δD and δL.

The dumbbells formed from the microemulsion (method 2) had a very low polydispersity in both L and D, with $\delta L/L \cong \delta D/D \cong 0.02$, particularly notable given the small size of the particles. This result suggests that dumbbell formation occurred suddenly, after which the dumbbells were coated.

Polydispersities for the larger dumbbells (method 1) after different controlled growth conditions are given in Table 1. During controlled growth, the polydispersity remained roughly constant except in the case of sample 1A for which an increase in polydispersity in L occurred early in the seeded growth process. This may have occurred due to the somewhat higher TEOS feed rate (the product of the TEOS concentration and the TEOS/EtOH solution feed rate) for this sample, which may have increased the ion concentration and thus the likelihood that new dumbbells would form. It should be noted that the measurement uncertainty for L was on the order of 2% (due mainly to the uncertainty of finding the centers of each sphere), therefore the numbers given for polydispersity in L represent an upper bound. The low polydispersities in L throughout the growth for samples 1B and 1C is strong evidence that no new dumbbells were formed during the shell-growth steps for these samples.

Another factor affecting the synthesis of lower-aspect-ratio dumbbells was second nucleation and the growth of small spheres onto the surface of the dumbbells. For sample 1A_1, some of the added small spheres grew onto the surface of 10% of the dumbbells (see Table 1). For this reason, growth on this sample was continued with spheres removed (sample 1A_2) which led to second nucleation. This problem was eliminated in sample 1B, for which the concentration in the TEOS feed was substantially reduced. In sample 1C_1, for which no additional small particles were added and higher concentrations of dumbbell seed particles were used, some second nucleation was observed. However, in sample 1C_2, for which the concentration in the TEOS feed was reduced, no second nucleation was observed. Second nucleation was not necessarily a problem as the newly nucleated particles could be separated from the dispersion via centrifugation.

As seen in Figure 1, the peak dumbbell (number) concentration using method 1 was roughly 45% after about 70 h, with about 5% variation from synthesis to synthesis and less than 5% statistical uncertainty. At this peak dumbbell fraction, the fraction of three and four particle clusters was still remarkably low (<5%). Simple models for diffusion and shear-induced aggregation predict a peak dumbbell fraction of less than 25%[40,41] and higher fractions of three and four particle clusters than those measured in our experiments. At a lower ammonia concentration (60 mL/L), dumbbells formed more slowly, and three-particle clusters formed relatively faster. For example, after 140 h, the dumbbell yield had peaked at roughly 25% with the number of three-particle clusters at roughly 10%. We speculate the dumbbell yield may be determined by the thickness of the double layer and local hydrodynamic conditions specific to dumbbells. We are currently investigating these unusual aggregation phenomena more systematically.

The dumbbell yield for method 2 was 20% also with a low fraction (∼5%) of larger aggregates. It may be possible to further optimize the dumbbell yield of method 2.

(37) Osseo-Asare, K.; Arriagada, F. J. *Colloids Surf.* **1990**, *50*, 321.
(38) Hinton, R. *Density gradient centrifugation*; Elsevier: North-Holland 1976.
(39) Crocker, J. C.; Grier, D. G. *J. Colloid Interface Sci.* **1996**, *179*, 298. Particle tracking routines were downloaded from Crocker J. C.; Weeks E. R.. Particle tracking using IDL. http://www.physics.emory.edu/~weeks/idl/.
(40) Smoluchowski, M. *Z. Phys. Chem.* **1917**, *92*, 129.
(41) Zeichner, G. R.; Showalter, W. R. *AIChE J.* **1977**, *23*, 243.

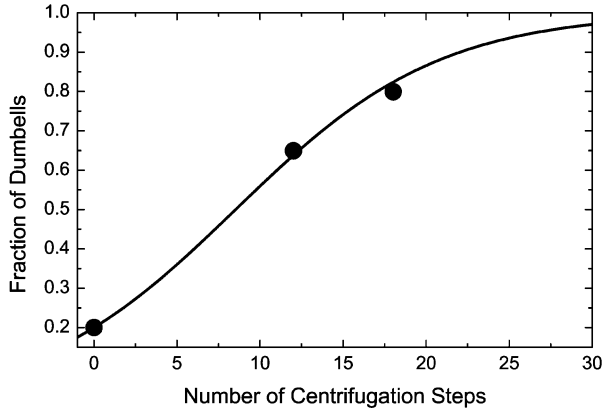

Figure 4. The increasing fraction of dumbbells using repeated centrifugation (sample 1B_1). The circles are experimental values. Centrifugation speeds of 1000 rpm were used with volume fractions of ~0.5%. The solid line is the theoretical fraction predicted by eq 1 with $f = 0.15$, where f is the fraction of singles removed with each step.

We were able to purify large quantities of dumbbells through repeated centrifugation in a uniform solvent. Beginning with a 20% dumbbell mixture containing very few three-particle clusters (<0.5%), the dumbbell fraction was increased to 85% after centrifuging 17 times. During the centrifugation, several samples were taken and the fraction of dumbbells measured.

This process of gradual purification of the dumbbells through repeated centrifugation can be modeled theoretically. Assuming that that a number fraction, f_s, of singles was removed at each step and that all of the dumbbells were retained in the sediment, a simple calculation gives the dumbbell fraction, $F(n)$, after n centrifugation steps:

$$F(n) = \frac{1}{1 + \left(\frac{1}{F(0)} - 1\right)(1 - f_s)^n} \tag{1}$$

This expression was fit to the data with f_s as the free parameter (Figure 4). Our result of $f_s = 0.15$ is reasonable, considering that we removed less than the maximum number of singles to ensure that no dumbbells were lost during each centrifugation step. In principle, this approach could provide large yields of pure dumbbells. Assuming the dumbbells sediment roughly 1.35 times as fast as single particles, the theoretical limit for f_s is 0.26. Inserting this into eq 1 suggests a highly purified sample could be achieved (>99% dumbbells) with 20 centrifugation steps for $F(0) = 0.2$ (although it would have taken 37 steps for $f_s = 0.15$).

Smaller yields (~several milligrams of colloids) of pure (>99%) dumbbell dispersions were achieved in one step through density gradient centrifugation.[38] This technique, while well established in a number of fields, has only recently been applied to large colloidal particles;[29] thus, we examine the optimal conditions in some detail here.

The theoretical limit for maximum loading of large, dense colloids, and thus optimum particle yield, can be calculated from simple considerations. In order for a liquid or complex fluid of nonuniform density to remain stable under a gravitational or centripetal force field, the fluid density must decrease with height,[38] i.e.

$$\frac{\partial \rho(z)}{\partial z} \leq 0 \tag{2}$$

Here, z is the height of the gradient, the origin of the z axis is at the top of the tube, and the direction of sedimentation (toward the bottom) is in the positive direction. If the fluid is a combination of colloids and a nonuniform solvent, we can express the density as

$$\rho = f_c \rho_c + (1 - f_c)\rho_s \tag{3}$$

where ρ is the total density, ρ_c is the density of the colloid particles (i.e., $\rho_c \approx 1.9$ g/mL in the case of silica[34]), $\rho_s = \rho_s(z)$ is the density of the nonuniform solvent, and $f_c = f_c(z)$ is the volume fraction of colloids. Assuming a linear gradient in density of the solvent, i.e., that $\rho_s(z) = ((\rho_1 - \rho_2)/\Delta z)z + \rho_2$, where ρ_1 is the solvent density at the top of the tube, ρ_2 is the solvent density at the bottom of the tube, and Δz the height of the gradient, the maximum gradient in the colloid fraction is found from eqs 2 and 3:

$$-\frac{\partial f_c}{\partial z} \leq \frac{\rho_2 - \rho_1}{\Delta z}\frac{1}{\rho_c - \rho_1} \tag{4}$$

Here we have assumed $f_c \ll 1$, which is the case for the dense colloids used in this paper. The maximum gradient in the colloid concentration is achieved when $\rho_2 - \rho_1$ is maximized. The optimal yield for a given colloid density, ρ_c, occurs when $\rho_c = \rho_2$, in which case $|\partial f/\partial z|_{max} = 1/\Delta z$. Using a sucrose solution with $\rho_2 = 1.34$ g/mL and $\rho_1 = 1.08$ g/mL, and a tube height of $\Delta z = 7$ cm, the maximum gradient is $|\partial f/\partial z|_{max} = 0.045$ cm^{-1}.

To calculate the optimal time for centrifugation, the sedimentation depth as a function of time was calculated for the gradient solution. The rate of sedimentation $v(z)$ at any given height depends on the solvent viscosity, $\eta(z)$, the solvent density, $\rho(z)$, the colloid effective radius, the centrifuge frequency, and ρ_c. Here we assume that the concentration of colloids is low enough that it is not a determining factor in $v(z)$. The total time to sediment from height z_i to z_f can be calculated numerically from the expression

$$t = \int_{z_i}^{z_f} \frac{1}{v(z)}\,dz \tag{5}$$

Using this expression, the position of the top and bottom of the colloid band as a function of time was calculated. This result was tested experimentally using 1.4 μm spheres in a sucrose solution with $\rho_2 = 1.30$ g/mL and $\rho_1 = 1.08$ g/mL, with the density, $\eta(z)$, taken from standard tables for sucrose in water solutions.[42] As seen in Figure 5, the theoretically predicted depth as a function of time and the band thickness match the experiment with no adjustable parameters.

An optimum centrifugation time was found by applying eq 4 to the case of bands of dumbbells and single particles. Equation 5 predicts a maximum in their separation, the ideal time for unloading the bands. As seen in Figure 6, this happens after 30 min of centrifugation at 1000 rpm with a starting position of 11 cm from the center of the centrifuge. Here it was assumed that the dumbbells sediment 1.2 times as fast as the spheres, a result that will vary slightly depending on the dumbbell aspect ratio. At this time, the thickness of the band has decreased by a factor of ~10 due to the strongly nonlinear increase of the viscosity with depth. This contraction increases the magnitude of the colloid concentration gradient $\partial f/\partial z$ in the band and must be taken into account when applying eq 3. Optimal results were obtained when using a

(42) Birnie, D. D.; Rickwood, D. Eds. *Centrifugal Separations in Molecular and Cell Biology*; Butterworth: London, Boston, 1978.

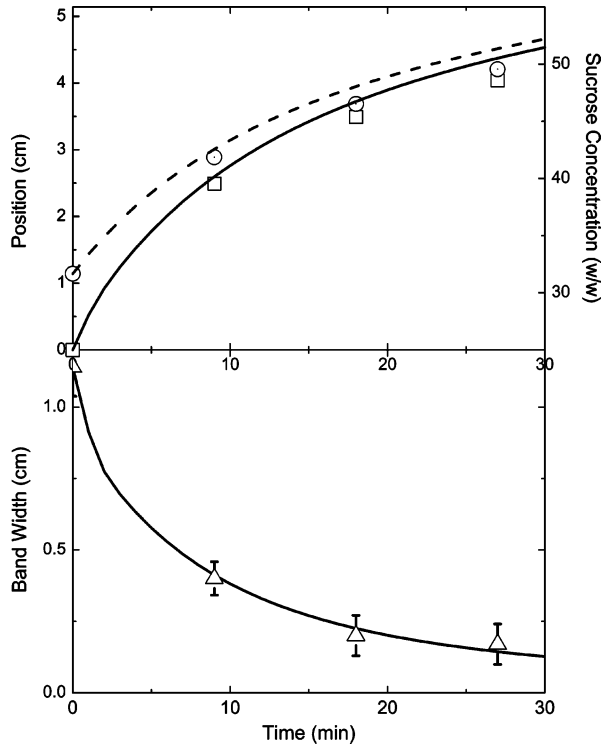

Figure 5. Theoretical (lines) and experimental (symbols) values of the band position (top) and width (bottom) during centrifugation of 1.4 μm spheres (loading concentration gradient of 0.005 (g/mL)/cm) at 1000 rpm. The position is the radial position of the band in the centrifuge relative to its position at the beginning of centrifugation. The top and bottom of the band are marked by the squares and circles (experimental) and the solid and dashed lines (theoretical), respectively. The right-hand side of the top plot gives the sucrose weight percentage in as a function of radius.

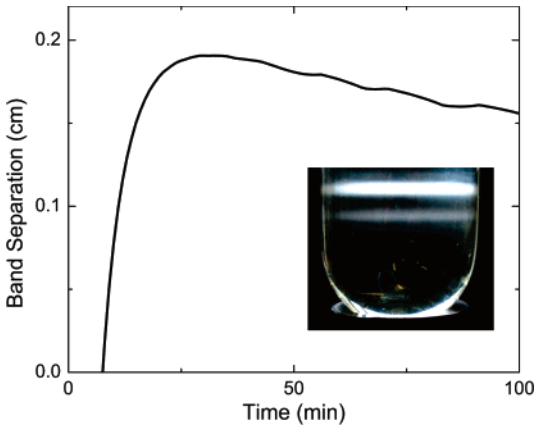

Figure 6. Theoretical prediction of the band separation vs time assuming a centrifuge speed of 1000 rpm and starting radius of 11 cm assuming that the dumbbells sediment 1.2 times as fast as the spheres. The theory predicts an optimum time to remove the bands. The inset shows a photograph of two bands formed after centrifugation for 20 min at 1000 rpm using sample 1B_2. The top band is composed of single spheres, the bottom dumbbells. The photo shows that the bands are clearly separated and can thus be separately removed. The bottom band is nearly index-matched with the sucrose solutions and is thus dimmer than the top band. There is also a very faint band of 3-particle aggregates which is not visible in this photo. The "ripples" in the theoretical curve are an artifact due to the limited resolution of the viscosity and density data for the sucrose solution.

centrifugation time slightly less than the theoretically optimal, for which the band thickness had decreased by

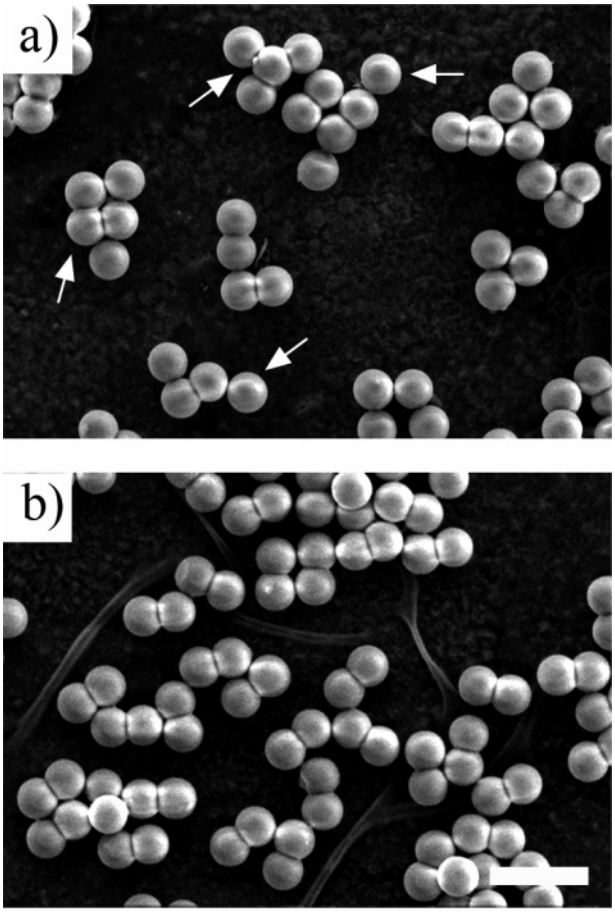

Figure 7. SEM image of sample 1A_1 before (a) and after (b) density gradient sedimentation. The arrows in (a) point to singles, a triple, and a quadruple particle. In the lower figure, only dumbbells remain. The scale bar in the lower right is 4 μm.

roughly a factor of ~5. Using this centrifugation time, the maximum allowed loading of the colloids in the top band was $|\partial f/\partial z|_{max} = 0.045/5 = 0.009$ cm^{-1}, producing a theoretical yield of 95 mg of dumbbells from a 40% dispersion (independent of particle size). Since this was more than sufficient for our measurements, we used somewhat lower colloid concentrations with net yields of ~15 mg. As seen in Figure 6, bands of single particles and dumbbells are clearly visible.

Figure 7 shows an SEM image of dumbbells before and after centrifugation. As seen in Figure 7a, a number of singles and a few triples and quadruples remained in the pre-centrifugation dispersion. After centrifugation, the dispersion contains only dumbbells (Figure 7b).

It can be difficult to distinguish between single spheres and dumbbells with scattering methods, except at small values of the scattered wavenumber. This was observed with X-ray scattering measurements of the small pure dumbbell samples grown from the microemulsion (method 2) and can be explained theoretically. The theoretical form factor for scattering from a dumbbell with $L/D = 1$, rotationally averaged, can be solved exactly using the Born approximation (single scattering).

$$F_{\text{dumbbell}} = F_{\text{sphere}}\left(1 + \frac{\sin(2qR)}{2qR}\right) \qquad (6)$$

where q is the wavenumber and R is the radius of the spheres forming the dumbbell, and F_{sphere} is the form factor from a Mie sphere calculation.[43,44] As seen in eq 6, F_{dumbbell}

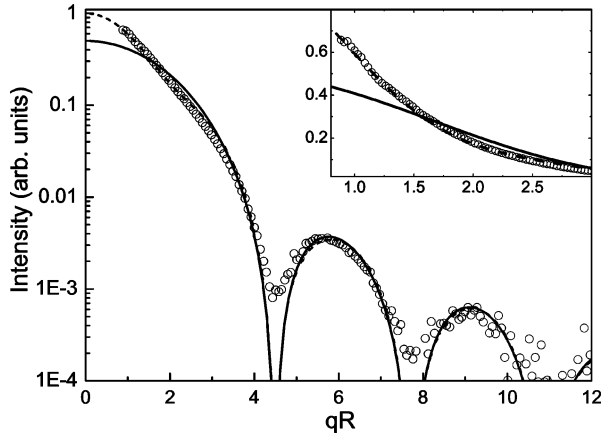

Figure 8. Intensity of scattered X-rays vs qR, where q is the wavenumber ($2\pi/\lambda$, where λ is the X-ray wavelength) and R is the radius of the spheres forming the dumbbell ($R = D/2$). The plot shows the measured data for a pure dumbbell sample with $D = 174$ nm. The inset shows the same data on a linear scale over a narrower range of wavenumbers. Also shown are the theoretical calculations for a dumbbell of aspect ratio 1 (dashed line), and for spheres of diameter 174 nm (solid line). As seen from the plot and the inset, the theory agrees well with the data. Also, it is clear that the main deviation of the dumbbell scattering from the prediction for spherical particles occurs at $qR < 4.5$, i.e., before the first minimum.

$\approx F_{\text{sphere}}$ for $qR \gg 1$. This makes small-angle X-ray scattering a particularly useful approach for examining dumbbell particles since low values of q can be resolved. As seen in Figure 8, the dumbbell dispersion is well modeled by eq 6. The result for pure dumbbells clearly deviates from the predicted result for spherical particles[44] before the first scattering minimum ($qR = 4.5$). The small discrepancies still visible may be related to the fact that the size ratio of these particles was not exactly 1 ($L/D = 0.80$) and/or the presence of a small amount of higher aggregates.

Sediments of several samples of fluorescently labeled dumbbells were observed in the confocal microscope. The individual cores could be located and tracked using methods similar to those described in refs 1 and 2. At low concentrations, the location and orientation of individual dumbbells were easily found (Figure 9a). At higher concentrations, this became difficult, since it was difficult to distinguish between two spheres that are part of the same dumbbell from two spheres that are in contact but belong to different dumbbells. The simplest method of distinguishing these two cases is to measure the distance between the core centers of the two spheres. This distance is slightly less when the cores belong to the same dumbbell, depending on the dumbbell aspect ratio. Thus, by finding all of the nearest-neighbor distances, the tracking software can locate the dumbbells. To this end, a short IDL program was written to connect cores that belong to the same dumbbell (Figure 9b). Once the cores belonging to the same dumbbell were determined, the position and orientation of all of the dumbbells in a three-dimensional sediment could be determined.

As the aspect ratio of the dumbbells approaches one, using the core separation distance to distinguish dumbbells becomes more difficult. The RITC-coated particles depicted in Figure 9c offer a potential solution to this problem. In this case, two channels were measured with the confocal microscope. An FITC channel yielded the position of the dumbbell cores. The RITC channel located the shells of the particles. As pointed out by the arrows in Figure 9c, the dumbbell particles have a reduced RITC signal between the cores compared with the signal between two touching cores. In this way, two cores in the same dumbbells may be distinguished from cores in neighboring, touching dumbbells. Another possibility to distinguish which cores belong to which dumbbell particles may be to use the fact that the dynamics of the cores that are attached is strongly correlated.

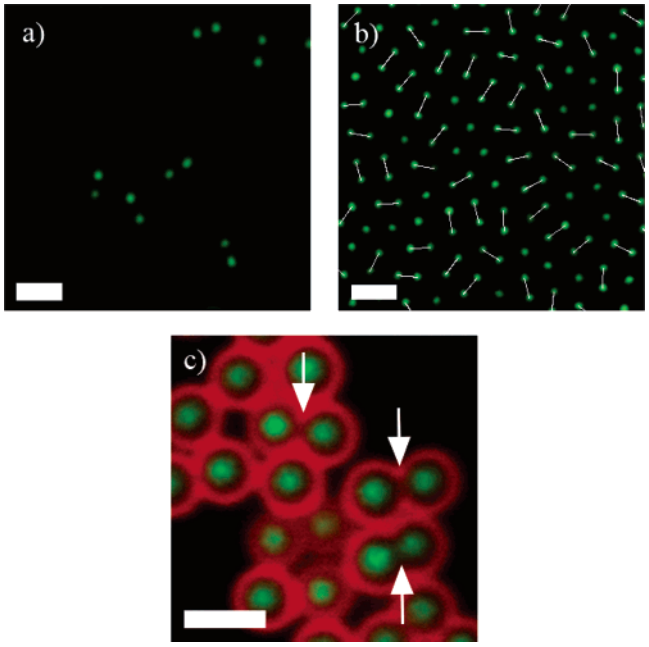

Figure 9. Scanning laser confocal microscopy photos of FITC (green)-labeled dumbbells (sample 1C_2) at low (a) and high (b) concentrations and of FITC core, RITC (red) shell dumbbells ((c) a sample made under similar conditions to sample 1B_3). At low concentrations (a), the position and orientation of individual dumbbells can be easily resolved. At high concentrations (b), the position and orientation of individual dumbbells, as denoted by the solid white lines, were found by pairing up cores that were separated by less than D using image analysis software (IDL) Some of the dumbbells in (b) are tipped up with respect to the glass so that the coupled core cannot be seen. The arrows in (c) point out the lack of RITC at the center of dumbbells. This lack of signal distinguishes a dumbbell from two touching spheres. The scale bars are (a) 3, (b) 3, and (c) 2 μm.

Conclusion

We have shown that it is possible to create highly monodisperse dispersions of anisotropic particles with well-defined aspect ratios from 0 to 1. The cores of these particles can be labeled to allow for confocal and fluorescent microscopy measurements and quantitative structural analysis in three dimensions. Future work includes the quantitative analysis of dense dispersions of these particles using confocal microscopy and light scattering techniques, characterization of crystalline and plastic crystalline phases, study of the effect of electric fields on dense dispersions of these particles, tuning the dumbbell interactions by changing the solvent properties, and modeling the effect of shear on the phase behavior. We are also investigating some of the anomalous aggregation phenomena encountered in this study.

Acknowledgment. We would like to thank Jacob Hoogenboom for synthesis of the FITC labled core−shell spheres, Diana Maas for the microemulsion synthesis and Christina Graf for additional 300 nm silica particles, and

(43) Imhof, A. private communication.
(44) Bohren, C. F.; Huffman D. R. *Absorption and Light Scattering by Small Particles*; John Wiley and Sons: New York, 1983.

Andrei Petukhov, Igor Dolbnya, Arnout Imhof, and Job Thijssen for helping us with X-ray scattering measurements at Grenoble, France (ESRF, BM26 DUBBLE-beamline) and the X-ray analysis. This work was financially supported by the Foundation for the Fundamental Research of Matter (FOM), which is part of The Netherlands Organization for Scientific Research (NWO). Additional support for one of the authors (P.M.J.) was provided by the Simmons College Fund for Research.

LA0518750